High-cholesterol diet fuels myeloma progression, dysregulates adipokine expression *in vivo*, and impairs treatment response *ex vivo*

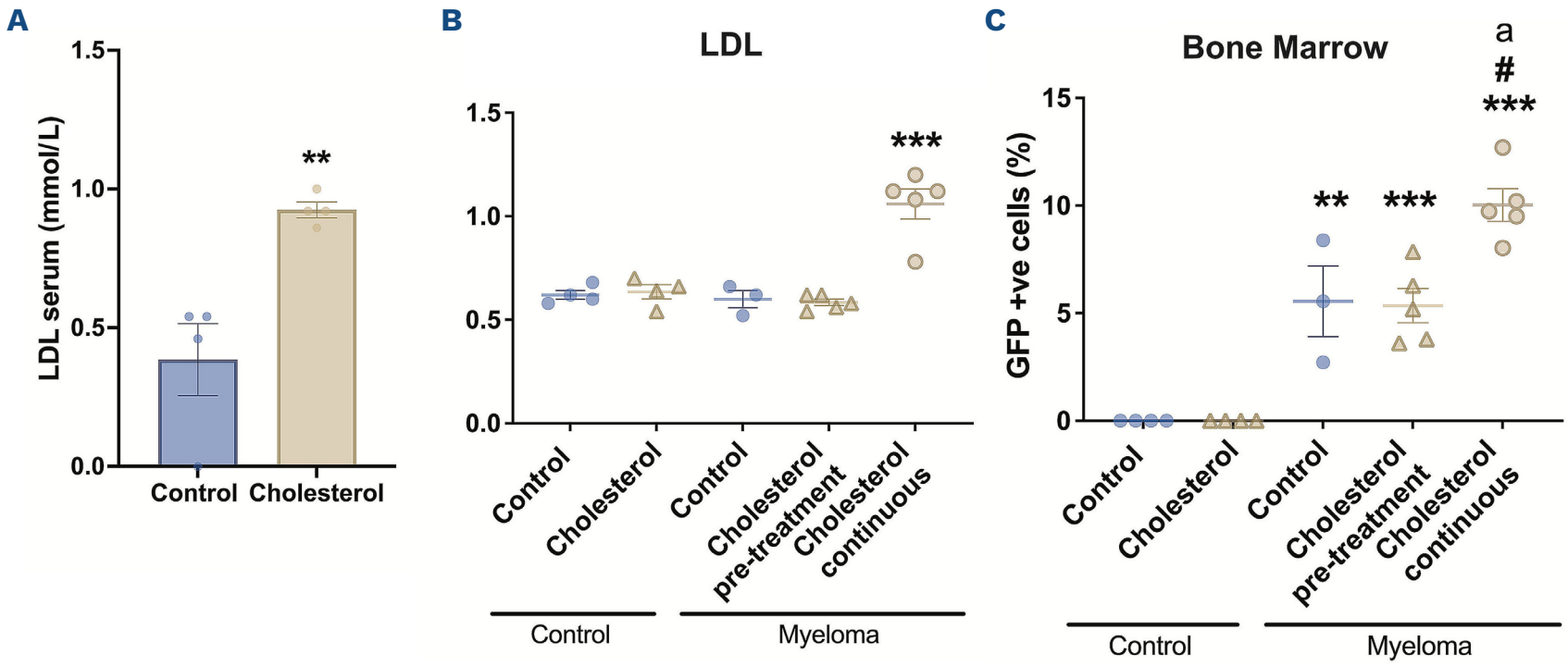
Multiple myeloma (MM) is an incurable hematologic cancer where malignant plasma cells accumulate in the bone marrow (BM).[1] MM evolves from the pre-malignant disorder monoclonal gammopathy of undetermined significance and despite recent advances in therapy, MM remains incurable largely due to drug resistance.[2] Obesity is the second leading cause of cancer and has been linked to several types of malignancies, including MM.[3,4] Although the exact mechanism by which obesity impacts MM pathogenesis is still unclear, it is the only modifiable risk known for MM and so it provides hope for dietary and lifestyle interventions.

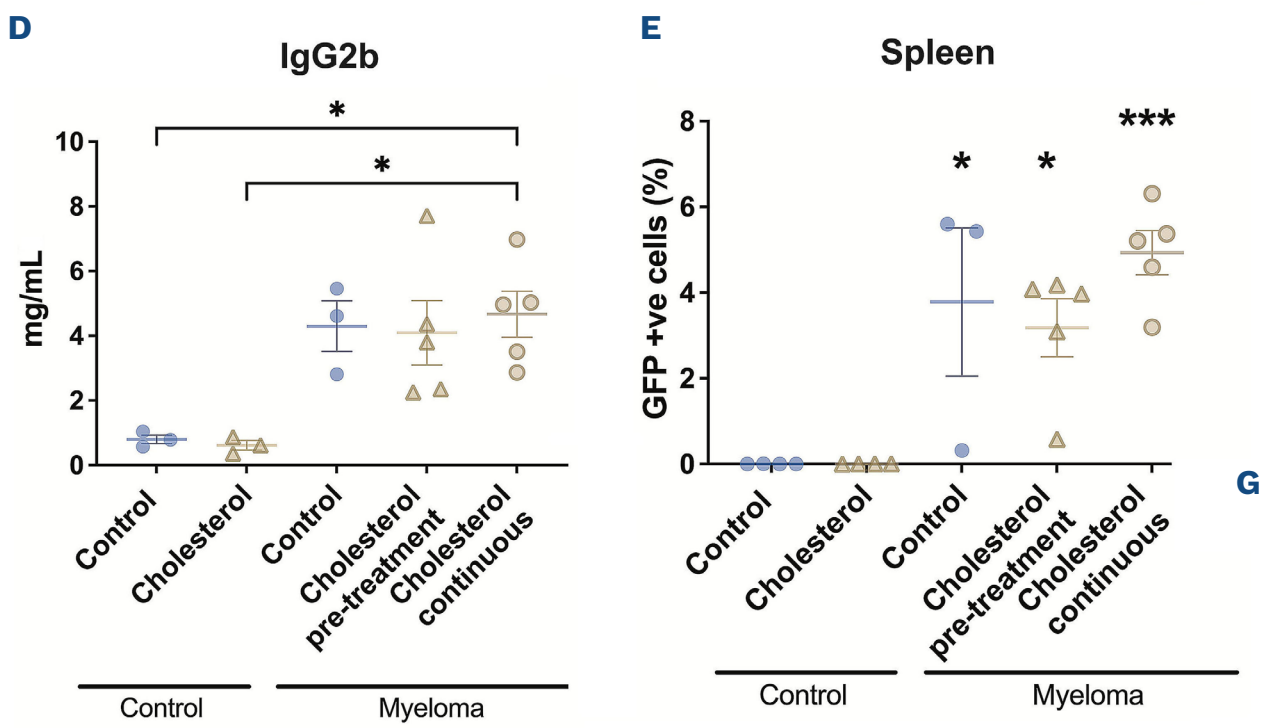
Strongly associated with obesity is high cholesterol. Several studies have shown that MM patients have a reduction in total cholesterol, low-density lipoproteins (LDL) and high-density lipoproteins (HDL) in plasma compared to healthy individuals with more evident changes in later stages of disease.[5,6] However, despite significant efforts to elucidate the role of total cholesterol or LDL in cancer, little is known about the effect of high circulating cholesterol and LDL levels in MM disease.

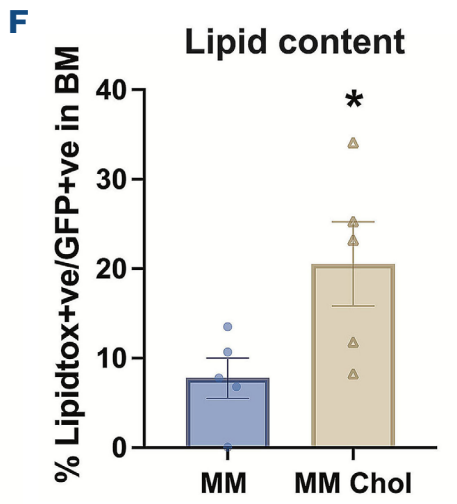
To understand the effect of cholesterol on myeloma progression *in vivo*, C57BL/KaLwRij mice were placed on a 2% cholesterol diet for 4 weeks after which time mice showed increased circulating LDL (Figure 1A; *Online Supplementary Figure S1A*) with no changes in body weight (*Online Supplementary Figure S1B*). Increased liver weight (*Online Supplementary Figure S1C, D*) and signs of fatty liver disease were seen (*data not shown*). Mice were then inoculated intravenously with 5TGM1-GFP cells and cholesterol diet was either halted at this point or maintained continuously (*Online Supplementary Figure S1A*). LDL levels remained elevated only in the animals fed continuously with the cholesterol diet (Figure 1B), which also showed a significant increase in tumor burden and serum paraprotein (IgG2β) levels compared to the myeloma control group (Figure 1C, D). No significant changes in spleen tumor burden or weight were detected in any of the cholesterol diet groups suggesting a bone-specific effect of LDL (Figure 1E; *Online Supplementary Figure S1E*). Myeloma cells from continuously cholesterol-fed animals had a higher proportion of highly lipidtox-positive cells demonstrating a higher intracellular lipid content (Figure 1F, G). Initiation of the cholesterol-enriched diet at the time of tumor inoculation (*Online Supplementary Figure S1A*) resulted in significantly higher BM tumor burden and bone lesions with no changes in spleen (Figure 1H-J). All animal procedures were conducted in accordance with the Animals Scientific Procedures Act of 1986 (UK) and approved by the University of Oxford Animal Welfare and Ethical Review Body (Home Office project licenses PCCCC8952 and PP9500304). Myeloma is heavily dependent on the BM microenvironment, therefore we investigated the impact of dietary cholesterol on local, as compared to systemic, factors. The very-low-density lipoprotein (VLDL)/LDL cholesterol fraction in BM plasma was increased in cholesterol-fed mice (Figure 2A). Using an adipokine proteome profiler we detected elevated levels of the adipokine resistin after cholesterol diet and in myeloma-bearing mice specifically in BM plasma (Figure 2B, C). We corroborated the increase in resistin by enzyme-linked immunosorbent assay, demonstrating a significant increase following cholesterol diet in BM plasma (Figure 2D) but not blood (Figure 2E). Interestingly, relative to all adipokines, resistin was one of the highest expressed adipokines in blood, but was reduced in BM plasma highlighting the differences in the local and systemic soluble milieu (*Online Supplementary Figure S2A, B*). Tumor-bearing mice showed significantly higher resistin in BM plasma (Figure 2F), with a positive correlation between BM plasma resistin and IgG2bκ in myeloma-bearing mice that was lost with cholesterol treatment (Figure 2G).

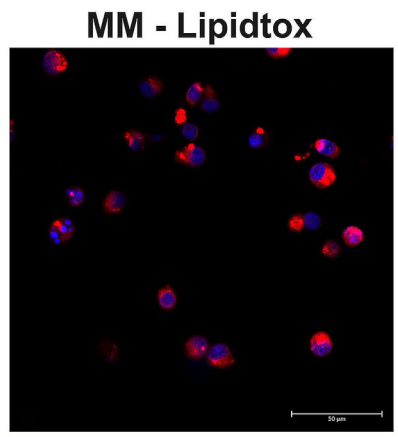
To further investigate the role of LDL in myeloma, we studied the effect of LDL on myeloma growth and drug resistance, focusing on the proteasome inhibitor bortezomib, following recent evidence for the sensitivity of bortezomib-resistant myeloma cells to a cholesterol-lowering drug.[10] LDL reversed the reduction in myeloma cell viability caused by delipidation or metabolic stress (no fetal bovine serum) (*Online Supplementary Figure S2C*). VLDL had no effect on viability of JJN3 or MM1S whereas in 5TGM1-GFP cells, VLDL had similar effects to LDL suggesting differential sensitivities of myeloma cells to lipid depletion and cholesterol levels (*Online Supplementary Figure S2C*). In support of this, lipid depletion and metabolic stress increased LDL uptake, with variability in uptake between cell lines (*Online Supplementary Figure S2D-G*). LDL was incorporated after 3 hours (Figure 3A) and completely blocked the effect of the proteasome inhibitor bortezomib to reduce viability in metabolically-stressed myeloma cells (*Online Supplementary Figure S3A, B*). LDL-treated BM isolated from myeloma-bearing mice was used *ex vivo*, showing the same level of protection from bortezomib (Figure 3B).

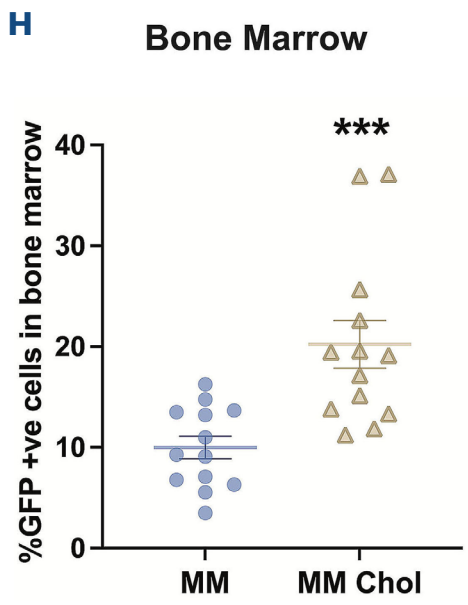
Bortezomib reduced viability and induced expression of apoptotic markers that was reversed upon addition of LDL prior to bortezomib treatment (Figure 3C). In cell cycle analysis, LDL also reduced the apoptotic fraction that was increased

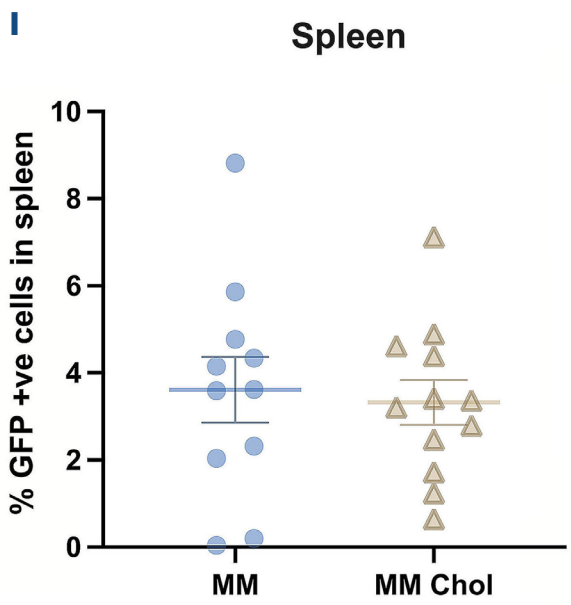


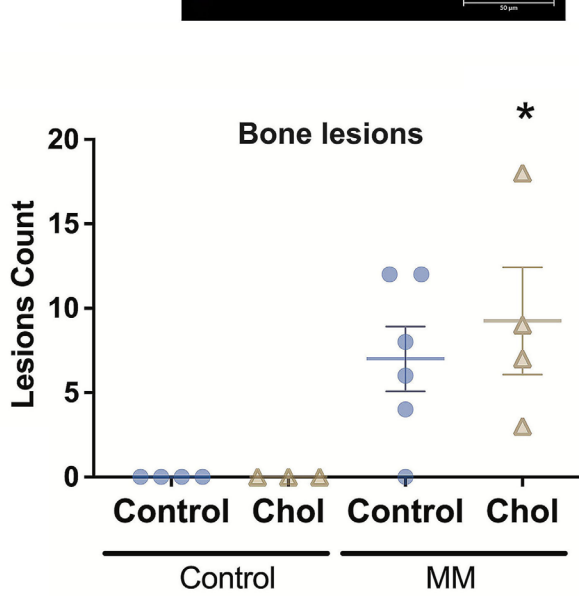












Continued on following page.

Figure 1. A high-cholesterol diet increases low-density lipoprotein and bone marrow tumor burden *in vivo* in C57BL/6 KaLwRij mice. (A) C57BL/6 KaLwRij mice were fed with either control or high cholesterol diet for 4 weeks and serum low-density lipoprotein (LDL) was measured. Mice were then randomly distributed into either control or tumor-bearing mice (myeloma) and inoculated with $1.5x10^6$ 5TGM1-GFP cells. Cholesterol non-tumor mice and cholesterol pre-treatment myeloma mice had cholesterol diet halted at time of inoculation. (B) LDL in serum was measured at endpoint. (C) Proportion of 5TGM1 GFP-positive (+ve) tumor cells in bone marrow (BM). (D) IgG2bκ levels in serum. (E) Proportion of GFP+ve myeloma cells in spleen. (F) Lipid content of GFP+ve myeloma cells from BM quantified by lipidtox stain and flow cytometry. (G) Representative image acquired by confocal microscopy showing incorporation of far-red lipidtox in JJN3. In separate experiments, cholesterol diet was given from time of inoculation and GFP+ve myeloma cells in BM (H) and spleen tumor burden (I) were quantitated by flow cytometry. (J) Number of bone lesions counted from micro-computed tomography images. For two-group comparison, two-tailed Student's *t* test was performed. **P*<0.05; ***P*<0.01 and ****P*<0.001. For more than 2 groups one-way anova analysis was performed. For (C), ***P*<0.01 and ****P*<0.001 compared to animals on control and cholesterol diets with no tumor. $^{\#\#}P$<0.01 compared to myeloma cholesterol pre-treatment and ^{a}P<0.05 compared to myeloma on control diet. For (E), **P*<0.05 and ****P*<0.001 compared to control with no tumor in control diet or cholesterol diet. If not otherwise indicated, **P*<0.05, ***P*<0.01 and ****P*<0.001 compared to control with no tumor. Results are presented as mean ± standard error of the mean.

following bortezomib treatment (*Online Supplementary Figure S3C*). Carfilzomib, MG132, metformin or dexamethasone were also tested, however LDL had no effect on drug response (*Online Supplementary Figure S2D-G*). To further investigate how LDL induces bortezomib resistance, we studied proteasome activity and performed cycloheximide chase assays. LDL-pretreated JJN3 myeloma cells had no change in proteasome activity after bortezomib treatment (Figure 3D; *Online Supplementary Figure S3H, I*).

Fluctuations in cholesterol accumulation can induce changes in plasma membrane fluidity and composition and can alter molecular pathways associated with drug uptake, efflux and chemoresistance, including caveolin-1.[7-9] Bortezomib induced a dose-dependent decrease in membrane fluidity in JJN3 myeloma cells. LDL-pretreated cells also exhibited a reduction in membrane fluidity but with no further changes following bortezomib treatment (*Online Supplementary Figure S3J*). LDL increased caveolin-1 expression in myeloma cells (*Online Supplementary Figure S4A*) and prevented the reduction in caveolin-1 and MDR1 expression induced by bortezomib (*Online Supplementary Figure S4B*). In support of this, bortezomib-resistant MM cells were found to have an increase in caveolin-1 and MDR1, alongside a decrease in INSIG1 which regulates cholesterol metabolism (*Online Supplementary Figure S4C*).

RNA-sequencing (RNA-Seq) was performed on JJN-3 myeloma cells in the presence and absence of LDL and bortezomib. Differentially expressed gene (DEG) analysis revealed changes in expression of genes key to cholesterol synthesis (e.g., *HMGCS1* or *INSIG1*) after bortezomib treatment, with LDL pretreatment restoring the transcriptomic profile of bortezomib-treated cells to that of control (Figure 3E; *Online Supplementary Figure S4D*). Accordingly, the PCA plot demonstrated a clear distinction of the bortezomib-treated group, and LDL pre-treated samples grouped together with the untreated (*Online Supplementary Figure S4E*). When gene set expression analysis (GSEA) hallmark gene sets were analyzed, the hallmark apoptosis gene set was enriched in bortezomib-treated cells compared to LDL-bortezomib-treated cells (*Online Supplementary Figure S4F*). GSEA revealed a significant effect of bortezomib on reactome cholesterol biosynthesis and cholesterol homeostasis (*Online Supplementary Figure S4G*). Further analysis using the ShinyGO tool and top 1,000 downregulated genes demonstrated proteasome pathway enrichment in bortezomib samples as compared to LDL-bortezomib-treated (*Online Supplementary Figure S5A*). Interestingly, ferroptosis was also among the most enriched pathways, demonstrated by both ShinyGO and GSEA (*Online Supplementary Figure S5A, B*). Only a small number of DEG were found after LDL treatment compared to untreated (*Online Supplementary Figure S5C, D*). ShinyGO analysis of all DEG revealed ferroptosis as one of only two modulated pathways (*Online Supplementary Figure S5E*) and GSEA using the WP ferroptosis gene set revealed a significant effect of LDL on ferroptosis in both control and bortezomib-treated cells (*Online Supplementary Figure S5A*).

Using data from the CoMMpass-MMRF database, a list of seven mevalonate pathway-related genes (M46454 human gene set, GSEA) was used to study whether their expression had an impact on probability of first response in patients. Expression of *HMGCR* and *HMGCS1*, key genes in the mevalonate pathway, had an effect in patients that were placed on bortezomib-based therapies as first option but not for other therapies, however differences were not significant after *P* value correction (*data not shown*). Further analysis studying the combined effect of both genes showed that they were determinant for the response to therapy only in patients under bortezomib therapy, demonstrating the importance of cholesterol metabolism in the response to bortezomib (Figure 3F, G).

In this study, high dietary cholesterol increased myeloma tumor burden in the BM, accompanied by increased lipid content in myeloma cells. Mice were fed standard chow diet supplemented with 2% cholesterol. Unlike a Western diet, which combines high fat, high sucrose, and added cholesterol to model obesity and metabolic syndrome, this approach isolates the specific contribution of cholesterol without the confounding effects of excess fat or sugar. Proteomic profiling revealed elevated resistin, an adipokine associated with both hypercholesterolemia and myeloma, positively correlating with IgG2β levels. Resistin therefore emerges as a potential biomarker and mediator of tumor-bone crosstalk.

Mechanistically, LDL-cholesterol induced resistance to the proteasome inhibitor bortezomib. Myeloma cells efficiently internalized LDL, which fully abrogated bortezomib-induced apoptosis and reversed its transcriptional signature, par-

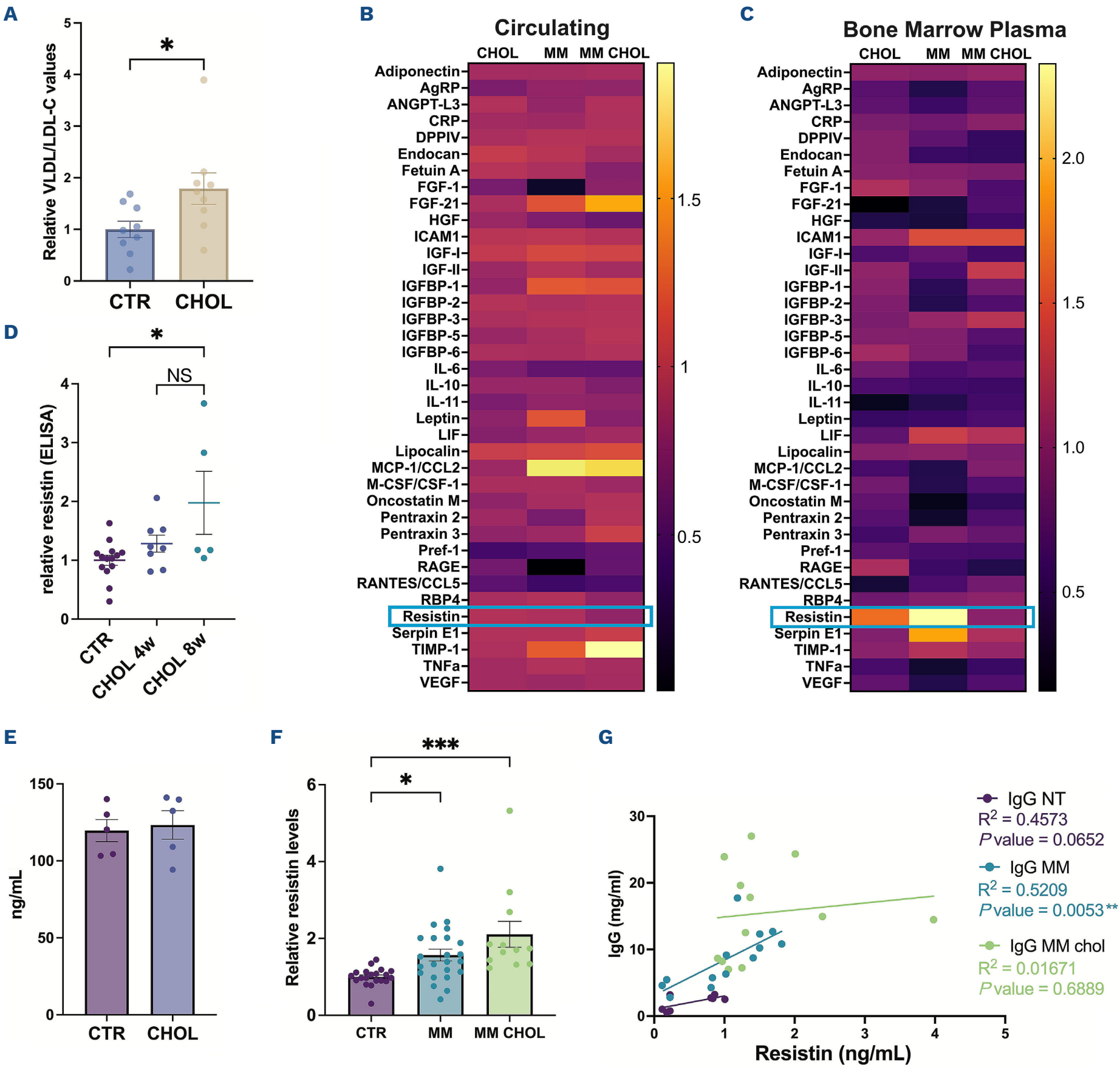
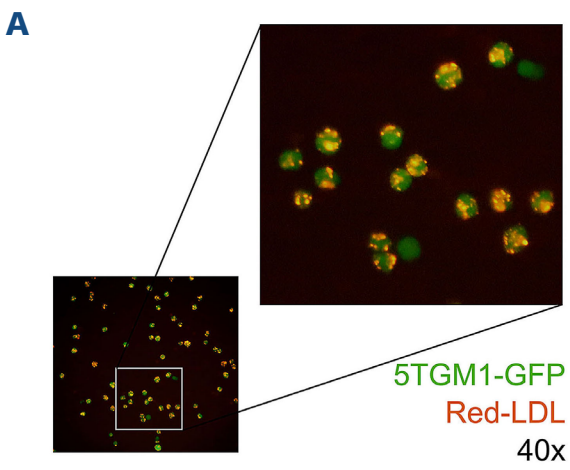
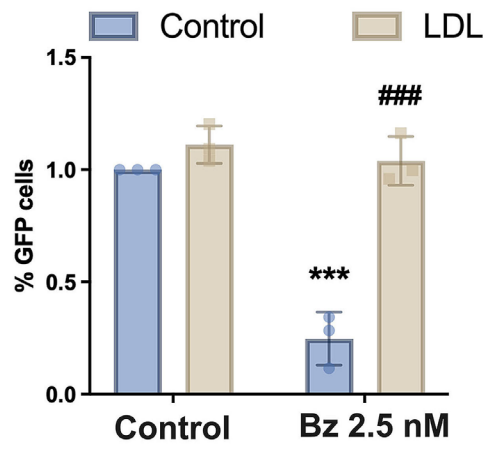
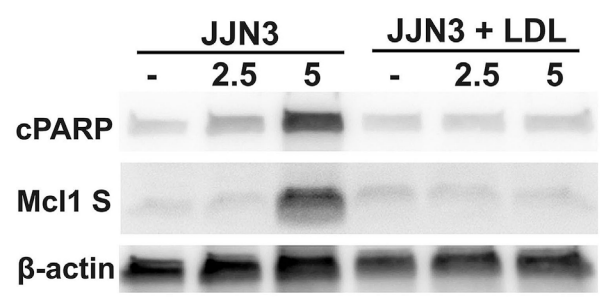
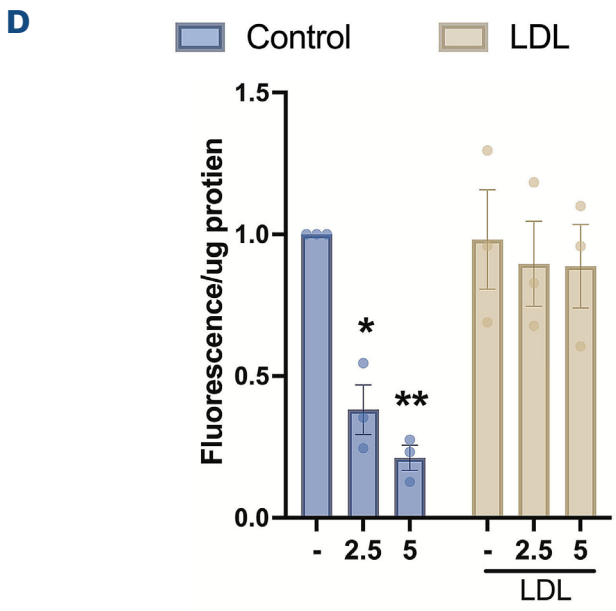


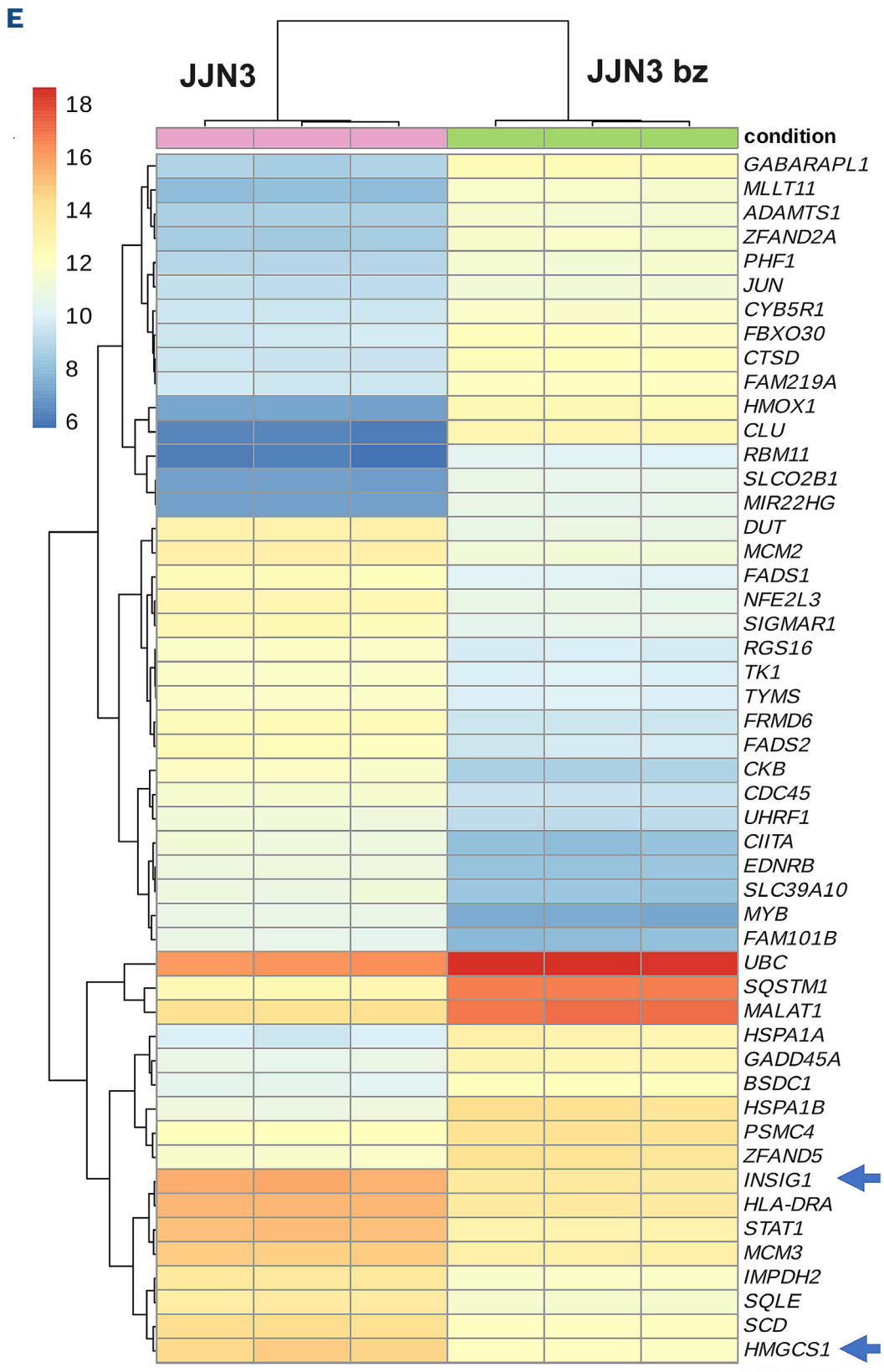
Figure 2. Adipokine profiles identify increased resistin in bone marrow in response to high cholesterol or myeloma. (A) Low-density/very-low-density lipoprotein C (LDL/VLDL-C) ratio in the bone marrow (BM) of C57BL/6 KaLwRij mice after 4 weeks of high cholesterol diet. Heat maps show relative expression of adipokines in blood (B) and bone marrow plasma (C) of a non-tumor mouse on cholesterol diet (CHOL), myeloma-bearing mouse (MM) and MM on cholesterol diet (MM CHOL) compared to non-tumor control. Cholesterol diet was given continuously in all groups. (D) Relative resistin expression (expressed as fold-increase compared to control) in BM plasma from non-tumor mice fed with control diet (CTR), cholesterol diet for 4 weeks (CHOL 4w) or cholesterol diet for 8 weeks (CHOL 8w). (E) Resistin expression in blood from control or cholesterol-fed animals for 8 weeks. (F) Relative resistin expression (expressed as fold-increase compared to control) in BM plasma in control non-tumor mice (CTR), MM and MM CHOL from inoculation. (G) Pearson correlation of IgG2bκ paraprotein and resistin levels in non-tumor mice in control diet (8 pairs of XY), tumor-bearing mice (13 pairs of XY) and tumor-bearing mice on cholesterol diet (12 pairs of XY). For 2 group comparison, two-tailed Student's *t* test was performed. For more than 2 groups one-way anova analysis was performed. If not otherwise indicated, **P*<0.05 and ****P*<0.001 compared to control. Results are presented as mean ± standard error of the mean.

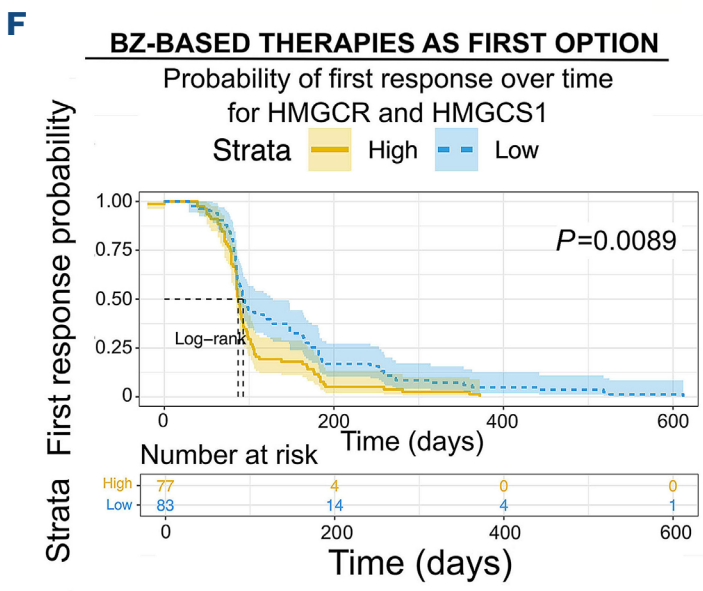


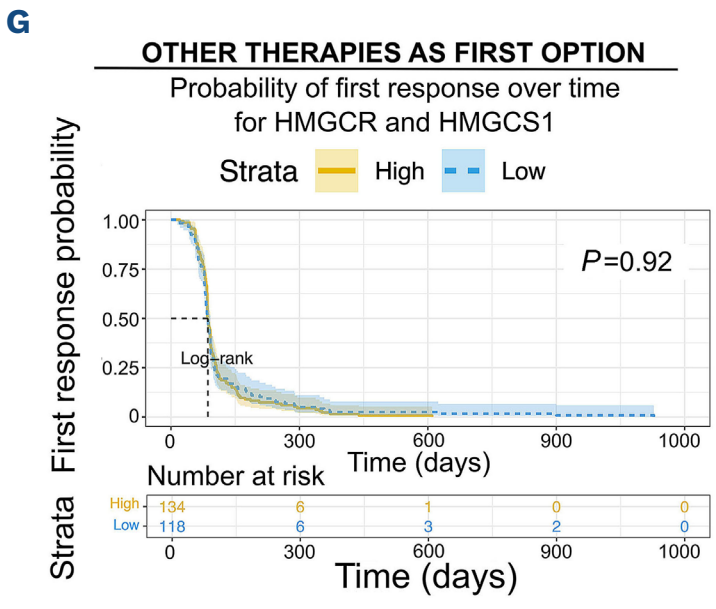












Continued on following page.

Figure 3. Low-density lipoprotein induces resistance to bortezomib and changes in the cholesterol pathway. (A) 5TGM1-GFP multiple myeloma (MM) cells were cultured in serum-free conditions and treated with pHrodo™ red-low-density lipoprotein (LDL) for 3 hours (h); 40x magnification. (B) Whole bone marrow (BM) was isolated from myeloma-bearing mice, seeded with no fetal bovine serum media and treated with 30 μg/mL LDL for 3 h before 24-h bortezomib treatment. Viability was quantitated by alamar blue (N=3). Tumor cell viability was assessed by flow cytometry as GFP-positive cells compared to control. (C) JJN3 were cultured in serum-free conditions ± LDL for 3 hours before bortezomib treatment for 24 h. Apoptotic markers cPARP and short Mcl-1 were measured by western blotting with concurrent viability quantitation. (D) JJN3 myeloma cells were treated in the presence and absence of LDL and bortezomib and proteasome activity measured using a proteasome 20S activity assay kit. (E) JJN3 myeloma cells were treated in the presence and absence of LDL and bortezomib and RNA-Seq performed. Heatmap showing differential expression gene (DEG) analysis from bortezomib *versus* control cells. CoMMpass study data analysis showing the impact of *HMGCR* and *HMGCS1* expression on the probability of first response over time in patients with bortezomib-based therapies as first option (F) and patients with other therapies (G). One-way ANOVA analysis was performed. For (B) ***P<0.001 compared to control non-LDL condition. For (B) ***P<0.001 compared to control non-bortezomib treated condition, ###P<0.001 compared to bortezomib treated no-LDL condition. For (D) *P<0.05, **P<0.01 compared to control (no bortezomib, no LDL). Results are presented as mean ± standard error of the mean.

ticularly under metabolic stress. This effect was specific to bortezomib. RNA-sequencing and enrichment analyses implicated ferroptosis in mediating drug resistance, consistent with evidence linking cholesterol to ferroptosis evasion and the ability of cholesterol-lowering agents to effectively inhibit bortezomib-resistant myeloma cells.[10]

Our *in vitro* data demonstrates that LDL pretreatment of myeloma cells altered membrane fluidity and increased caveolin-1 expression, a protein linked to redox homeostasis, adhesion and bortezomib resistance.[11] Modulation of membrane fluidity may influence not only intracellular trafficking and therapeutic response but also the diapedesis of myeloma cells, potentially modulating myeloma cell homing to the BM. *In silico* patient analysis using the MMRF CoMMpass study data supported these findings: the level of expression of key genes in the mevalonate pathway (*HMGCS1, HMGCR*) predicted outcomes only in patients with bortezomib-based therapy as a first option.

Resistin was elevated in the BM niche following high cholesterol, consistent with the cholesterol-oriented metabolism of BM adipocytes.[12] Known to induce multidrug tolerance through ABC transporter upregulation, resistin may contribute to bortezomib resistance.[13-15]

In summary, our findings reveal the impact of high cholesterol on myeloma progression and bortezomib resistance and provide insight into the cellular mechanisms that underly this, identifying resistin as a potential mediator within the tumor-bone microenvironment. Furthermore, our studies provide important mechanistic insight to facilitate optimal pharmacological or dietary intervention strategies.

Authors

Beatriz Gámez,[1,2] Danielle J. Whipp,[1] Srinivasa R. Rao,[1,2] Emma V. Morris,[1] Young Eun Park,[1,2] Zeynep Kaya[1] and Claire M. Edwards[1-3]

[1]Nuffield Department of Surgical Sciences, University of Oxford; [2]Oxford Translational Myeloma Center, University of Oxford and [3]Nuffield Department of Orthopedics, Rheumatology and Musculoskeletal Sciences, University of Oxford, Oxford, UK

Correspondence:
C.M. EDWARDS - claire.edwards@ndorms.ox.ac.uk

https://doi.org/10.3324/haematol.2025.288286

Received: June 16, 2025.
Accepted: February 2, 2026.
Early view: February 12, 2026.

©2026 Ferrata Storti Foundation
Published under a CC BY license

Disclosures

No conflicts of interest to disclose.

Contributions

BG and CME conceived the experiments. BG planned the experiments. BG and DJW performed the experiments. BG analyzed the data. SR contributed to sample preparation and analyzed RNA-seq data. ZK, EVM and YP contributed to *in vivo* work and sample preparation. BG and CME wrote the manuscript.

Acknowledgments

We are grateful to the Multiple Myeloma Research Foundation Personalized Medicine Initiatives (https://research.themmrf.org and www.themmrf.org).

Funding

This research was funded by Blood Cancer UK (20004 and 15026), Rosetrees, Cancer Research UK, the National Institute for Health Research (NIHR) Oxford Biomedical Research Center (BRC) and funds from the CRRMF and Equality and Diversity Unit (University of Oxford). The views expressed are those of the author(s) and not necessarily those of the NHS, the NIHR or the Department of Health.

Data-sharing statement

RNA-sequencing data from this article is available from the authors upon request.

References

1. Kumar SK, Rajkumar V, Kyle RA, et al. Multiple myeloma. Nat Rev Dis Primers. 2017;3:17046.
2. Malard F, Neri P, Bahlis NJ, et al. Multiple myeloma. Nat Rev Dis Primers. 2024;10(1):45.
3. Morris EV, Edwards CM. Bone marrow adipose tissue: a new player in cancer metastasis to bone. Front Endocrinol (Lausanne). 2016;7:90.
4. Morris EV, Edwards CM. Adipokines, adiposity, and bone marrow adipocytes: Dangerous accomplices in multiple myeloma. J Cell Physiol. 2018;233(12):9159-9166.
5. Yavasoglu I, Tombuloglu M, Kadikoylu G, Donmez A, Cagirgan S, Bolaman Z. Cholesterol levels in patients with multiple myeloma. Ann Hematol. 2008;87(3):223-228.
6. Hungria VT, Latrilha MC, Rodrigues DG, Bydlowski SP, Chiattone CS, Maranhao RC. Metabolism of a cholesterol-rich microemulsion (LDE) in patients with multiple myeloma and a preliminary clinical study of LDE as a drug vehicle for the treatment of the disease. Cancer Chemother Pharmacol. 2004;53(1):51-60.
7. Kozalak G, Butun I, Toyran E, Kosar A. Review on bortezomib resistance in multiple myeloma and potential role of emerging technologies. Pharmaceuticals (Basel). 2023;16(1):111.
8. Chan NN, Yamazaki M, Maruyama S, et al. Cholesterol is a regulator of CAV1 localization and cell migration in oral squamous cell carcinoma. Int J Mol Sci. 2023;24(7):6035.
9. Zhao X, Lian X, Xie J, Liu G. Accumulated cholesterol protects tumours from elevated lipid peroxidation in the microenvironment. Redox Biol. 2023;62:102678.
10. Zhang H, Wang H, Hu Y, et al. Targeting PARP14 with lomitapide suppresses drug resistance through the activation of DRP1-induced mitophagy in multiple myeloma. Cancer Lett. 2024;588:216802.
11. Zhan D, Du Z, Zhang S, et al. Targeting caveolin-1 in multiple myeloma cells enhances chemotherapy and natural killer cell-mediated immunotherapy. Adv Sci (Weinh). 2024;12(4):e2408373.
12. Attane C, Esteve D, Chaoui K, et al. Human bone marrow is comprised of adipocytes with specific lipid metabolism. Cell Rep. 2020;30(4):949-958.e946.
13. Kim HJ, Lee YS, Won EH, et al. Expression of resistin in the prostate and its stimulatory effect on prostate cancer cell proliferation. BJU Int. 2011;108(2 Pt 2):E77-83.
14. Kuo CH, Chen KF, Chou SH, et al. Lung tumor-associated dendritic cell-derived resistin promoted cancer progression by increasing Wolf-Hirschhorn syndrome candidate 1/Twist pathway. Carcinogenesis. 2013;34(11):2600-2609.
15. Pang J, Shi Q, Liu Z, et al. Resistin induces multidrug resistance in myeloma by inhibiting cell death and upregulating ABC transporter expression. Haematologica. 2017;102(7):1273-1280.